

# S

1

## 2 SEAFLOOR HEAT FLOW: METHODS AND 3 OBSERVATIONS

4 Earl E. Davis<sup>1</sup> and Andrew T. Fisher<sup>2</sup>

5 <sup>1</sup>Geological Survey of Canada, Sidney, BC, Canada

6 <sup>2</sup>University of California at Santa Cruz, Santa Cruz,  
7 CA, USA

### 8 Definitions

9 *Heat flow.* The rate of thermal energy transfer in a medium  
10 driven either conductively along a thermal gradient or  
11 advectively via mass transport. The standard unit is  
12 watts, W. The term is also used to describe a subdiscipline  
13 of geophysics, as in the title of this entry.

14 *Conductive heat flux.* The heat flow per unit area diffusing  
15 by conduction along a thermal gradient, determined as the  
16 product of the thermal gradient and thermal conductivity.  
17 The standard unit is  $W\ m^{-2}$ . The term *heat flow density*  
18 has been used correctly as a synonym; the term *heat flow*,  
19 traditionally but inexactly used as a synonym for heat flux,  
20 more strictly applies to the integrated heat flux over  
21 a specified area or region (watts).

22 *Advective heat flux.* The rate of heat transfer per unit area  
23 carried by a moving medium, proportional to the velocity  
24 and the heat capacity of the medium. The standard unit is  
25  $W\ m^{-2}$ .

26 *Thermal conductivity.* The quantity that defines the ability  
27 of a medium to transfer heat by steady-state diffusion. The  
28 standard unit is  $W\ m^{-1}\ K^{-1}$ .

29 *Hydrothermal circulation.* Large-scale pore-fluid convec-  
30 tion driven by thermal buoyancy, in which fluid flux and  
31 advective heat flux are strongly influenced by the perme-  
32 ability structure of the host formation.

### History of observations

33

Pioneering measurements of temperature below the sea- 34  
floor (e.g., Petterson, 1949; Revelle and Maxwell, 1952; 35  
Bullard, 1954) were made to compare the thermal state 36  
of the ocean crust with that of continents and thus to 37  
improve the knowledge of the present-day heat loss from 38  
the Earth. The early data demonstrated that gravity-driven 39  
probes and corers that penetrated a few meters into sea- 40  
floor sediments could provide meaningful geothermal gra- 41  
dients, and they provided a foundation for the marine heat 42  
flow discipline. Methods for measuring the seafloor ther- 43  
mal gradient and thermal conductivity (the product of 44  
which is conductive heat flux) improved in subsequent 45  
years, the number and geographic distribution of determi- 46  
nations increased, and patterns of seafloor heat flux were 47  
gradually revealed. Initially, the average seafloor heat flux 48  
appeared to be similar to that through continents, despite 49  
the contribution from crustal radiogenic heat production, 50  
which is significant in the continental crust but not in the 51  
oceanic crust. Heat-flux values over midocean ridges were 52  
found to be significantly higher on average than in the 53  
flanking basins, but locally, values were often inexplica- 54  
bly scattered (Von Herzen and Uyeda, 1963; Lee and 55  
Uyeda, 1965). Higher heat flux at midocean ridges was 56  
consistent with emerging ideas about seafloor spreading, 57  
although the values measured were lower than expected 58  
from early theoretical models for the formation of ocean 59  
lithosphere. For nearly 2 decades, regionally low and 60  
scattered seafloor heat-flux values remained unexplained. 61

By the 1970s, studies began to be done with improved 62  
navigation, and with more closely spaced measurements 63  
made in the context of local sediment and igneous crustal 64  
structure. Results provided a sound basis for the hypoth- 65  
esis that hydrothermal circulation in the igneous crust and 66  
advective loss through unsedimented igneous outcrops 67  
caused both the scatter and the lower-than-expected 68  
values in young areas (Lister, 1972). Further 69

70 improvements to instrumentation and observational strategies, in particular the development of probes that could be used with great efficiency for multiple measurements during a single instrument lowering, and the practice of making measurements in the context of geologic structure, led to the use of heat flux in the study of the process of hydrothermal circulation itself (Williams et al., 1974). With this new knowledge, it was possible to decipher the variability in measurements in a way that could lead to a better quantification of deep-seated heat flux, the goal of the original marine heat flow studies, and to understand the hydrologic processes behind the perturbations. Thus began a diverse range of applications of marine heat flow over a broad range of scales. A summary of the suite of tools currently in use for these studies is provided in the next section, along with a brief description of how heat-flux determinations are made. This is followed by a few examples of data from specific studies that illustrate how data are used, and a summary of some of the major conclusions that have been made through such studies.

## 90 Methods

### 91 Shallow measurements in marine sediments

92 Heat flux through the seafloor is often determined using temperatures measured with a series of sensors mounted on the outside of gravity-driven corers (Figure 1a), and thermal conductivities measured on the recovered sediment cores. Depths of penetration in excess of 10 m can be achieved in soft sediment, providing a valuable check on potential perturbations from bottom-water temperature variations, although accuracy is often limited by physical disturbances caused by the coring process, by changes in the physical properties of the recovered material, by incomplete recovery, and by the imperfect depth registration between the cores and the intervals between the temperature sensors. Probes devoted exclusively to heat-flux measurements are typically limited to lengths of a few meters, but they have several distinct advantages. They allow thermal conductivity to be measured under in situ conditions and at depths that are co-registered with temperature measurements, and they allow transects of many measurements to be made efficiently during single instrument lowerings. A typical multipenetration heat-flux probe (Figure 1b) employs a heavy strength member that resists bending during repeated penetration and withdrawal from the sediment, and a small-diameter, rapidly responding tube containing thermistor sensors and a linear heater element. In situ temperatures are estimated by extrapolating transient decays following probe penetration, and conductivities are determined from the rate of change of temperature following steady or impulsive activation of the heater. A typical data record is shown in Figure 2, as are the resulting determinations of temperature and thermal conductivity. Heat flux is determined as the linear regression fit of temperature versus cumulative thermal resistance,  $R$ :

$$R = \sum [\Delta z / \lambda(z)]$$

125 where  $\lambda$  is thermal conductivity measured at a series of depths,  $z$ , and  $\Delta z$  is the depth interval assumed to be represented by each measurement. This is equivalent to calculating heat flux as the product of thermal gradient and the harmonic mean of thermal conductivity between temperature measurements, as was done in early marine heat flow studies. Errors associated with possible bottom-water temperature variations are evaluated by examining systematic deviations from linearity as a function of the number of thermistors included in the fit, working progressively up toward the shallowest measurement point. Complete descriptions of instruments and discussions of data reduction methods can be found in Lister (1979); Hyndman et al. (1979); Davis (1988), Wright and Loudon (1989), and Villinger and Davis (1987).

### 140 Deep borehole measurements

141 Where observations are needed in hard formations or at depths greater than can be penetrated with a gravity-driven device, drilling is required. For research objectives, this has been done primarily through the Deep Sea Drilling Project, the Ocean Drilling Program, and the Integrated Ocean Drilling Program. In relatively unconsolidated sediments (typically the uppermost 50–100 m below the seafloor), hydraulically driven piston corers are deployed from the bottom of the drill string, and temperatures are measured at the tip of the core barrel (Horai and Von Herzen, 1985). At greater depths below the seafloor, high-strength probes can be pushed in with the weight of the drill string sufficiently far below the bottom of the hole (c. 1 m) to gain an unperturbed measurement (Uyeda and Horai, 1980; Davis et al. 1997a) (Figure 1c). Deeper than a few hundred meters in sediment, or at any level in crystalline rock, bottom-hole measurements are not feasible; instead, long-term borehole measurements are required to discriminate the natural formation thermal state from the commonly large and long-lived perturbations from drilling and subsequent fluid flow into or out of the hole. The most reliable method for determining the natural thermal state of crustal rocks has been to seal holes and install thermistor strings for long-term monitoring (Davis et al., 1992) (Figure 3).

## 166 Example studies

### 167 Bottom-water temperature perturbations

168 Seafloor heat-flux measurements rely on the assumption that both long- and short-term bottom-water temperature variations are small; the volume of ocean bottom water is very large and the temperature of the source in polar regions is regulated by the formation of sea ice. Many early measurements were made with temperatures determined at only three depths over a span of a few meters, however. Good checks on the validity of this assumption were not possible until temperature observations began to be made in deep-sea boreholes and long records of

178 bottom-water temperature were acquired (Hyndman et al.,  
179 1984; Davis et al., 2003). An ideal suite of observations  
180 that would allow errors associated with bottom-water tem-  
181 perature variations to be quantified throughout the world's  
182 oceans – one that is broadly distributed both geographi-  
183 cally and with ocean depth – does not yet exist, but the  
184 available data show that gradients measured a few meters  
185 below the seafloor generally do permit accurate determi-  
186 nations of heat flux in large areas of the oceans where  
187 depths are greater than  $\sim 2,000$  m. One example where  
188 errors are demonstrated to be small is illustrated in  
189 Figure 4, where closely colocated seafloor probe and bore-  
190 hole observations are compared. Significant bottom-water  
191 temperature variations are ruled out by the linearity of  
192 the plots of temperature versus cumulative thermal  
193 resistance, and by the agreement between the shallow  
194 probe and deep borehole determinations. This illustration  
195 also shows the importance of precise colocation when  
196 doing such a comparison, given the local spatial variabil-  
197 ity of heat flux as defined by neighboring probe  
198 measurements.

199 A more direct approach uses observations of bottom-  
200 water fluctuations. An example from a 5,000-m-deep site  
201 in the western Atlantic (Figure 5a) shows that in this area,  
202 oceanographic perturbations might have a modest influ-  
203 ence on measured gradients. Estimated gradient perturba-  
204 tions at depths of less than 2–3 m below the seafloor range  
205 up to  $10 \text{ mK m}^{-1}$  (Figure 5b), that is, up to 20% of the geo-  
206 thermal gradient if the heat flux were  $50 \text{ mW m}^{-2}$ . A sec-  
207 ond example from a 2,600-m-deep site in the eastern  
208 Pacific shows smaller variability (Figure 5c), although  
209 perturbations estimated at a depth of 2 m could still result  
210 in a heat-flux determination error of up to 10%. Observa-  
211 tions like these are clearly useful for guiding measurement  
212 strategy (e.g., depth of penetration) wherever heat flux is  
213 low and precise determinations are required.

#### 214 Heat-flux signals from hydrothermal circulation

215 Hydrothermal circulation is a major source of error when  
216 determinations of deep-seated heat flux are sought, but it  
217 is also an important geological process. Hence it has been  
218 the focus of a large number of studies. Instructive exam-  
219 ples of the influence of hydrothermal circulation are  
220 shown in Figure 6, where closely spaced measurements  
221 were made along transects striking perpendicular to base-  
222 ment structure. The first (Figure 6a) is in an area where  
223 sediment cover is continuous over a broad region span-  
224 ning several tens of kilometers. Locally, heat flux varies  
225 inversely with sediment thickness. Such variations are  
226 common in areas of young seafloor, but can occur across  
227 relatively old seafloor as well (Embley, 1980; Von Herzen,  
228 2004; Fisher and Von Herzen, 2005). They are the conse-  
229 quence of thermally efficient, local convection in perme-  
230 able igneous rocks beneath low-permeability sediment  
231 cover. If the permeability of the igneous “basement” for-  
232 mation is high, vigorous convective flow maintains nearly  
233 constant temperatures at the sediment/basement interface

234 despite variations in the thermal resistance of the overlying  
235 sediment layer. In this instance, the average seafloor  
236 heat flux is close to that expected from the underlying litho-  
237 sphere, suggesting that from a thermal perspective, the  
238 circulation in the upper igneous crust is sealed in by the  
239 extensive sediment cover. The second transect  
240 (Figure 6b) crosses a sediment-covered area immediately  
241 adjacent to an area of outcropping igneous crust (where  
242 measurements are impossible). Local variations like those  
243 in Figure 6a are present, but even more apparent is a sys-  
244 tematic variation of a larger scale, with heat flux increas-  
245 ing with distance from the area of basement outcrop,  
246 opposite to the expected trend of decreasing heat flux with  
247 increasing seafloor age. Temperatures estimated at the top  
248 of the igneous section increase systematically as well,  
249 suggesting that heat is transported laterally by fluid circula-  
250 tion and mixing in the sediment-sealed igneous crust.  
251 Heat exchange between the well-ventilated and sedi-  
252 ment-sealed areas, indicated by the heat-flux deficit in this  
253 example, suggests a lateral heat-transfer scale of 20 km.  
254 Examples elsewhere suggest that the effects of advective  
255 heat loss may be felt laterally as far as 50–100 km (e.g.,  
256 Fisher et al., 2003).

257 Ever since the early work of Lister (1972), the mere  
258 presence of local variability has been used as  
259 a diagnostic indicator of hydrothermal circulation in both  
260 young and old areas (e.g., Figure 6c), but with widely  
261 spaced observations, neither of the signals exemplified  
262 in Figure 6a and b could be resolved coherently; values  
263 were simply scattered and averages were often low. When  
264 systematic, detailed transects of observations began to be  
265 completed in context of colocated seismic data, the vigor  
266 of the convection could be inferred quantitatively from  
267 the nonconductive thermal regime (Fisher and Becker,  
268 1995; Davis et al. 1997b), and the amount of heat lost from  
269 the crust by fluid advection could be estimated with grow-  
270 ing confidence (e.g., Anderson and Skilbeck, 1980; Stein  
271 and Stein, 1994; Harris and Chapman, 2004).

272 Two major lessons are learned from detailed observa-  
273 tions like these for drawing conclusions about deep-seated  
274 heat flux. First, to ensure that observations do not suffer  
275 from the bias caused by convective ventilation, it must  
276 be demonstrated that there are no exposures of permeable  
277 rock at faults or volcanic edifices within distances of sev-  
278 eral tens of kilometers. Second, large numbers of closely  
279 spaced observations must be made, ideally colocated with  
280 seismic reflection data, so that the local variability can be  
281 understood and meaningfully averaged, and the locally  
282 relevant lateral transport scale can be assessed (e.g.,  
283 Sclater et al., 1976; Davis et al., 1999).

284 Lessons learned about the way that the seawater inter-  
285 acts with the oceanic crust are far-reaching and contin-  
286 uously expanding. Estimates for the temperatures of  
287 circulation, the chemistry of the fluids, the volumetric rates  
288 of exchange between the crust and the ocean, and the con-  
289 sequent effects on crustal alteration and ocean chemistry  
290 have become reasonably well understood (e.g., Mottl and  
291 Wheat, 1994; Elderfield and Schultz, 1996). Studies of

[AU1]

292 the actual distribution of crustal permeability, the percent-  
 293 age of rock affected by hydrothermal alteration, and the  
 294 potential for chemosynthetic microbial populations are  
 295 the focus of current investigations.

#### 296 Dependence of heat flux on age and the global 297 average

298 With the potentially large influence of hydrothermal circula-  
 299 tion in mind, it is clear that a simple compilation of heat-  
 300 flux data will provide a deceiving view of global heat loss.  
 301 Except in old ocean basins, values are likely to be  
 302 scattered and low relative to the heat loss expected from  
 303 the underlying lithosphere. But by taking only those mea-  
 304 surements that are sufficiently far from known permeable  
 305 crustal outcrops and sufficiently numerous to provide  
 306 a reliable local average, a subset of data can be gathered  
 307 that provides a reliable determination of deep-seated heat  
 308 flux. When considered in the context of lithospheric age,  
 309 the results have been found to be consistent with both  
 310 the characteristics of age-dependent seafloor subsidence  
 311 and with simple lithospheric cooling theory (see entry on  
 312 Oceanic Lithosphere: Thermal Structure). In young areas,  
 313 heat flux is found to decline linearly with the inverse  
 314 square root of age, following the simple relationship  
 315  $Q = C t^{-1/2}$  (where  $Q$  is heat flux in  $\text{mW m}^{-2}$ ,  $t$  is age in  
 316 Ma, and  $C$  is a constant estimated between 475 and 510;  
 317 Lister et al., 1977; Harris and Chapman, 2004). High-  
 318 quality observations in older regions ( $>100$  Ma) are gen-  
 319 erally uniform, in the range of 45–50  $\text{mW m}^{-2}$  (Lister  
 320 et al., 1990), suggesting that the thermal structure of the  
 321 lithosphere may become stabilized in a state regulated  
 322 either by the convectively supplied heat flux from the  
 323 underlying asthenosphere, or by the combination of  
 324 a compositionally established lithospheric thickness and  
 325 the relatively uniform temperature of the vigorously  
 326 convecting asthenosphere.

327 With the relationship between heat flux and age thus  
 328 defined, the problems of the unknown bias and large scat-  
 329 ter in young areas and the sparse distribution of measure-  
 330 ments in large portions of the oceans can be overcome.  
 331 A reliable estimate for the total heat flow through the floor  
 332 of the ocean can be had by using the area/age relationship  
 333 for the oceans defined by seafloor magnetic anomalies  
 334 (e.g., Parsons, 1982; Wei and Sandwell, 2006), along with  
 335 a robust heat-flux/age relationship. Several such estimates  
 336 have been made (e.g., Williams and Von Herzen, 1974;  
 337 Sclater et al., 1980; see summary in Jaupart et al., 2007),  
 338 and all fall in a relatively narrow range centered around  
 339 32 TW (with contributions from marginal seas and hot-  
 340 spot swells included). This yields an average seafloor flux  
 341 of roughly  $107 \text{ mW m}^{-2}$ , a number that has little physical  
 342 significance, but is considerably greater than that esti-  
 343 mated in the early days of marine heat flow, and greater  
 344 than the average though continents (c.  $67 \text{ mW m}^{-2}$ ),  
 345 particularly when the latter is adjusted for the contribution  
 346 of continental crustal radiogenic heat (c.  $33 \text{ mW m}^{-2}$ ).

With the total heat flow thus constrained, the heat lost  
 advectively by ventilated circulation can be estimated  
 from the difference between this and the age-binned aver-  
 age of unfiltered observations. Such estimates of this “heat  
 deficit” fall in the neighborhood of 10 TW (Stein and  
 Stein, 1994; Harris and Chapman, 2004). Most of this def-  
 icit occurs in seafloor less than 8–10 Ma in age, and it  
 becomes insignificant on average by an age of 65 Ma.  
 The actual age at which advective loss becomes insignifi-  
 cant is locally variable, depending primarily on the conti-  
 nuity of accumulating sediments that bury the igneous  
 crust (Anderson and Skilbeck, 1980; Harris and Chapman,  
 2004), and the associated increase in spacing between  
 basement outcrops that are essential for hydrothermal  
 recharge and discharge on older ridge flanks (Fisher and  
 Wheat, 2010).

#### The signature of subduction

Marine heat flux is used extensively to constrain deep  
 thermal structure in studies of continental margins and  
 marginal basins. A transect crossing the forearc prism of  
 the Cascadia subduction zone illustrates one such applica-  
 tion (Figure 7). This transect begins with standard gravity-  
 driven probe measurements over the incoming plate and  
 outermost accretionary prism, where bottom-water tem-  
 perature variability is small. Where the seafloor is  
 shallower than 1,500–2,000 m, other measurement tech-  
 niques are used, including borehole measurements and  
 estimates made using the depth to a bottom-simulating  
 seismic reflector (BSR), which marks the limit of meth-  
 ane-hydrate stability. This reflector defines a unique set  
 of pressure-temperature conditions, and with constraints  
 on seismic velocity and thermal conductivity of the sec-  
 tion above the BSR, the thermal gradient and heat flux  
 can be estimated. Alternatively, a small set of seafloor  
 heat-flux measurements can be used as a “calibration.”  
 In either case, the travel-time depth to BSRs can serve as  
 a widespread proxy for thermal data (e.g., Yamano et al.,  
 1982). This technique is valuable where bottom-water  
 temperature variability is too large to permit accurate  
 heat-flux determinations with shallow probes, where sed-  
 iments are too hard to allow probe penetration, or where  
 there are few conventional measurements. Observations  
 like these allow the thermal structure to be inferred deep  
 within subduction zones, providing a critical constraint  
 on the rheology of the rocks and the potential for  
 seismogenic slip along the subduction thrust interface. In  
 the example shown (Figure 7), the seafloor heat flux is  
 variable locally, but regional values and trends are consis-  
 tent with the expected thermal state of the thickly  
 sedimented subducting plate.

In another study of the subducting Cocos Plate seaward  
 of the Middle America Trench, variations in the thermal  
 state of the plate are strongly influenced by regional differ-  
 ences in hydrothermal heat loss, and these correlate with  
 differences in seismic processes occurring at depth  
 (Newman et al., 2002; Fisher et al., 2003). One part of

AU2

403 the plate is extensively cooled by hydrothermal circulation  
 404 before the Cocos Plate is subducted, and earthquakes  
 405 observed within the subduction wedge in this area are relatively  
 406 deep (>20 km). Earthquakes tend to be shallower  
 407 (<20 km) along an adjacent segment of the subduction  
 408 zone, where there is no evidence for regional advective  
 409 heat extraction. One explanation for the different earth-  
 410 quake depths is that cooling of part of the Cocos Plate  
 411 slows dewatering and the transition of smectite to illite  
 412 in subducting sediments (Spinelli and Saffer, 2004).  
 413 Illite-rich sediments are more likely to undergo brittle  
 414 deformation at depth, so the delay in heating associated  
 415 with hydrothermal circulation in the crust prior to subduc-  
 416 tion causes a landward shift of the locked region where  
 417 earthquakes are most likely to occur.

#### 418 Summary

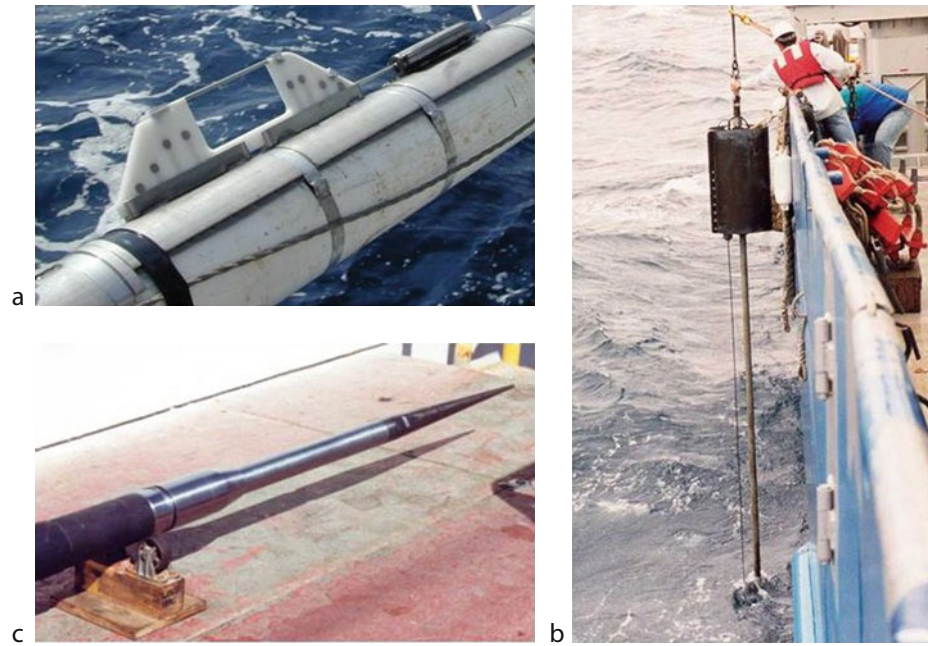
419 Seafloor heat flux can be measured with high accuracy in  
 420 most deep-ocean settings with gravity-driven probes that  
 421 penetrate a few meters into seafloor sediment. Improve-  
 422 ments in heat-flux measurement technology, improve-  
 423 ments in navigation, and integration with swath  
 424 bathymetric, seismic, and other data that provide geologi-  
 425 cal context for heat-flux measurements have greatly  
 426 advanced our understanding of many global, regional,  
 427 and local heat flow processes. Comparison of seafloor  
 428 and borehole data has demonstrated that measurements  
 429 made with short probes are accurate, provided that bot-  
 430 tom-water temperature variations are relatively small.  
 431 Compilations of global heat-flux data show that heat flux  
 432 tends to vary systematically with seafloor age, following  
 433 a  $t^{-1/2}$  relation, at least until seafloor age exceeds  
 434 100 Ma, after which heat flux tends to become relatively  
 435 constant. Determining the deep-seated lithospheric heat  
 436 flux requires quantification of the potentially large influ-  
 437 ence of hydrothermal circulation in the permeable igneous  
 438 rocks of the upper oceanic crust. This is best accomplished  
 439 through closely spaced transects of heat-flux measure-  
 440 ments collocated with seismic reflection profiles that con-  
 441 strain the hydrologic structure, and regional maps that  
 442 allow identification of basement outcrops. This approach  
 443 has been applied in numerous settings, providing valuable  
 444 constraints on the flow of water within the oceanic crust,  
 445 the exchange of water, heat, and solutes between the crust  
 446 and the oceans, the formation of hydrothermal mineral  
 447 deposits, the accumulation of gas hydrates, and the devel-  
 448 opment and maintenance of a subseafloor microbial bio-  
 449 sphere. Individual heat-flux measurements and transects  
 450 of measurements can be extended across broad regions  
 451 using the depth to bottom-simulating seismic reflectors.  
 452 These and other applications were never imagined by  
 453 those who developed the original techniques for acquisi-  
 454 tion of seafloor heat-flux data 6 decades ago, but they  
 455 illustrate how acquiring this kind of data has remained  
 456 valuable for multidisciplinary studies of thermal,  
 457 hydrogeologic, tectonic, and microbiological conditions  
 458 and processes within the lithosphere.

#### Bibliography

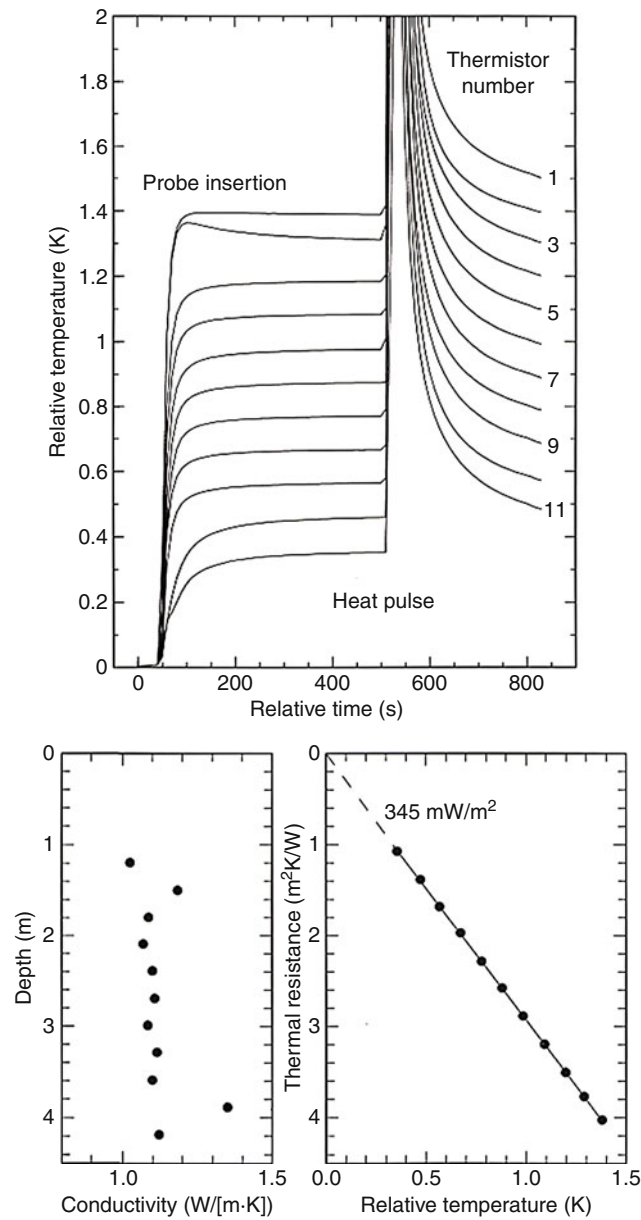
- Anderson, R. N., and Skilbeck, J. N., 1980. Oceanic heat flow. In 460  
 Emiliani, C. (ed.), *The Sea*. New York: Wiley Interscience, 461  
 Vol. 7, pp. 489–523. 462
- Bullard, E. C., 1954. The flow of heat through the floor of the Atlan- 463  
 tic Ocean. *Proceedings of the Royal Society A*, **222**, 408–429. 464
- Davis, E. E., Wang, K., He, J., Chapman, D. S., Villinger, H., and 465  
 Rosenberger, A., 1997a. An unequivocal case for high Nusselt 466  
 number hydrothermal convection in sediment-buried igneous 467  
 oceanic crust. *Earth and Planetary Science Letters*, **146**, 468  
 137–150. 469
- Davis, E. E., 1988. Oceanic heat-flow density. In Haenel, R., 470  
 Rybach, L., and Stegena, L. (eds.), *Handbook of Terrestrial 471  
 Heat-Flow Density Determination*. Dordrecht: Kluwer, 472  
 pp. 223–260. 473
- Davis, E. E., Becker, K., Pettigrew, T., and Carson, B., 1992. 474  
 CORK: a hydrologic seal and downhole observatory for deep- 475  
 sea boreholes. *Proceedings ODP, Init. Repts.* 139, pp 45–53. 476
- Davis, E. E., Villinger, H., Macdonald, R. D., Meldrum, R. D. J., 477  
 and Grigel, J., 1997b. A robust rapid-response probe for measur- 478  
 ing bottom-hole temperatures in deep-ocean boreholes. *Marine 479  
 Geophysical Researches*, **19**, 267–281. 480
- Davis, E. E., Chapman, D. S., Wang, K., Villinger, H., Fisher, A. T., 481  
 Robinson, S. W., Grigel, J., Pribnow, D., Stein, J. S., and 482  
 Becker, K., 1999. Regional heat flow variations and implications for 483  
 the sedimented Juan de Fuca Ridge eastern flank: constraints on 484  
 lithospheric cooling and lateral hydrothermal heat transport. 485  
*Journal of Geophysical Research*, **104**, 17675–17688. 486
- Davis, E. E., Wang, K., Becker, K., Thomson, R. E., and Yashayaev, I., 487  
 2003. Deep-ocean temperature variations and implications for 488  
 errors in seafloor heat flow determinations. *Journal of Geophys- 489  
 ical Research*, **108**, 2034, doi:10.1029/2001JB001695. 490
- Elderfield, H., and Schultz, A., 1996. Mid-ocean ridge hydrother- 491  
 mal fluxes and the chemical composition of the ocean. *Annual 492  
 Review of Earth and Planetary Sciences*, **24**, 191–224. 493
- Embley, R. W., Hobart, M. A., Anderson, R. N., and Abbott, D., 494  
 1983. Anomalous heat flow in the northwest Atlantic: a case 495  
 for continued hydrothermal circulation in 80-M.y. crust. *Journal 496  
 of Geophysical Research*, **88**, 1,067–1,074. 497
- Fisher, A. T., and Becker, K., 1995. The correlation between heat 498  
 flow and basement relief: observational and numerical examples 499  
 and implications for upper crustal permeability. *Journal of 500  
 Geophysical Research*, **100**, 12,641–12,657. 501
- Fisher, A. T., and Von Herzen, R. P., 2005. Models of hydrothermal 502  
 circulation within 106 Ma seafloor: Constraints on the vigor of 503  
 fluid circulation and crustal properties below the Madeira Abyssal 504  
 Plain. *Geochemistry, Geophysics, Geosystems*, **6**, 505  
 doi:10.1029/2005GC001013. 506
- Fisher, A. T., and Wheat, C. G., 2010. Seamounts as conduits for 507  
 massive fluid, heat and solute fluxes on ridge flanks. *Oceanogra- 508  
 phy*, **23**(1), 74–87. 509
- Fisher, A. T., Stein, C. A., Harris, R. N., Wang, K., Silver, E. A., 510  
 Pfender, M., Hutnak, M. C., Cherkaoui, A., Bodzin, R., and 511  
 Villinger, H., 2003. Abrupt thermal transition reveals hydrother- 512  
 mal boundary and role of seamounts within the Cocos plate. 513  
*Geophysical Research Letters*, **30**(11), 1550, doi:10.1029/ 514  
 2002GL016766. 515
- Harris, R. N., and Chapman, D. S., 2004. Deep-seated oceanic heat 516  
 flux, heat deficits, and hydrothermal circulation. In Davis, E. E., 517  
 and Elderfield, H. (eds.), *Hydrogeology of the Oceanic Litho- 518  
 sphere*. New York: Cambridge University Press, pp. 311–336. 519
- Horai, K., and Von Herzen, R. P., 1985. Measurement of heat flow 520  
 on Leg 86 of the Deep Sea Drilling Project, in *Init. Repts., DSDP 521  
 86*, pp 759–777. 522

AU3

523	Hyndman, R. D., 1984. Review of Deep Sea Drilling Project geo-	566
524	thermal measurements through Leg 71. <i>Init. Repts. DSDP 78B</i> ,	567
525	pp 813–823.	568
526	Hyndman, R. D., Davis, E. E., and Wright, J. A., 1979. The mea-	569
527	surement of marine geothermal heat flow by a multipenetrating	570
528	probe with digital acoustic telemetry and in situ thermal conduc-	571
529	tivity. <i>Marine Geophysical Researches</i> , <b>4</b> , 181–205.	572
530	Hyndman, R. D., and Wang, K., 1993. Thermal constraints on the	573
531	zone of major thrust earthquake failure: the Cascadia subduction	574
532	zone. <i>Journal of Geophysical Research</i> , <b>98</b> , 2039–2060.	575
Au4	533 Jaupart, C., Labrosse, S., and Mareschal, J.-C., 2007. Temperatures,	576
534	heat, and energy in the mantle of the Earth. In Bercovici, D. (ed.),	577
535	<i>Treatise on Geophysics</i> . Elsevier Vol. 7, pp 253–303.	578
Au5	536 Lee, W. H. K., and Uyeda, S., 1965. Review of heat flow data in Lee,	579
537	W. H. K. (ed.), <i>Terrestrial Heat Flow, Geophysical Monograph 8</i> ,	580
538	Washington: American Geophysical Union, pp 87–190.	581
539	Lister, C. R. B., 1972. On the thermal balance of a mid-ocean ridge.	582
540	<i>Geophysical Journal International</i> , <b>26</b> , 515–535.	583
541	Lister, C. R. B., 1979. The pulse-probe method of conductivity mea-	584
542	surement. <i>Geophysical Journal of Royal Astronomical Society</i> ,	585
543	<b>57</b> , 451–461.	586
544	Lister, C. R. B., Sclater, J. G., Davis, E. E., Villinger, H., and	587
545	Nagihara, S., 1990. Heat flow maintained in ocean basins of	588
546	great age: investigations in the north-equatorial west Pacific.	589
547	<i>Geophysical Journal International</i> , <b>102</b> , 603–630.	590
548	Mottl, M. J., and Wheat, C. G., 1994. Hydrothermal circulation	591
549	through mid-ocean ridge flanks: fluxes of heat and magnesium.	592
550	<i>Geochimica et Cosmochimica Acta</i> , <b>58</b> , 2,225–2,237.	593
551	Newman, A. V., Schwartz, S. Y., Gonzalez, V., DeShon, H. R.,	594
552	Protti, J. M., and Dorman, L. M., 2002. Along-strike variability	595
553	in the seismogenic zone below Nicoya Peninsula, Costa Rica.	596
554	<i>Geophysical Research Letters</i> , <b>29</b> , 1–4, doi:10.1029/	597
555	2002GL015409.	598
556	Parsons, B., 1982. Causes and consequences of the relation between	599
557	area and age of the ocean floor. <i>Journal of Geophysical</i>	600
558	<i>Research</i> , <b>87</b> , 289–303.	601
559	Petterson, H., 1949. Exploring the bed of the ocean. <i>Nature</i> , <b>4168</b> ,	602
560	468–470.	603
561	Revelle, R. R., and Maxwell, A. E., 1952. Heat flow through the	
562	floor of the eastern North Pacific Ocean. <i>Nature</i> , <b>170</b> , 199–202.	
563	Sclater, J. G., Crowe, J., and Anderson, R. N., 1976. On the reliabil-	
564	ity of ocean heat flow averages. <i>Journal of Geophysical</i>	
565	<i>Research</i> , <b>81</b> , 2,997–3,006.	
	Sclater, J. G., Jaupart, C., and Galson, D., 1980. The heat flow	566
	through oceanic and continental crust and the heat loss of the	567
	earth. <i>Reviews of Geophysics</i> , <b>18</b> , 269–311.	568
	Spinelli, G. A., and Saffer, D., 2004. Along-strike variations in	569
	underthrust sediment dewatering on the Nicoya margin, Costa	570
	Rica related to the updip limit of seismicity. <i>Geophysical</i>	571
	<i>Research Letters</i> , <b>31</b> , 1–5, doi:10.1029/2003GL018863.	572
	Stein, C. A., and Stein, S., 1994. Constraints on hydrothermal heat	573
	flux through the oceanic lithosphere from global heat flow. <i>Jour-</i>	574
	<i>nal of Geophysical Research</i> , <b>99</b> , 3,081–3,095.	575
	Uyeda, S., and Horai, K., 1980. Heat flow measurements on Deep	576
	Sea Drilling Project Leg 60, in <i>Init. Repts., DSDP 60</i> , pp 789–	577
	800, Washington, U. S. Govt. Printing Office.	578
	Von Herzen, R. P., and Uyeda, S., 1963. Heat flow through the east-	579
	ern Pacific Ocean floor. <i>Journal of Geophysical Research</i> , <b>68</b> ,	580
	4,219–4,250.	581
	Villinger, H., and Davis, E. E., 1987. A new reduction algorithm for	582
	marine heat flow measurements. <i>Journal of Geophysical</i>	583
	<i>Research</i> , <b>92</b> , 12,846–12,856.	584
	Von Herzen, R. P., 2004. Geothermal evidence for continuing	585
	hydrothermal circulation in older (> 60 M.y.) ocean crust. In	586
	Davis, E. E., and Elderfield, H. (eds.), <i>Hydrogeology of the</i>	587
	<i>Oceanic Lithosphere</i> . Cambridge: Cambridge University Press,	588
	pp. 414–447.	589
	Wei, M., and Sandwell, D., 2006. Estimates of heat flow from Ceno-	590
	zoic seafloor using global depth and age data. <i>Tectonophysics</i> ,	591
	<b>417</b> , 325–335.	592
	Williams, D. L., and Von Herzen, R. P., 1974. Heat loss from the	593
	earth: new estimate. <i>Geology</i> , <b>2</b> , 327–330.	594
	Williams, D. L., Von Herzen, R. P., Sclater, J. G., and Anderson,	595
	R. N., 1974. The Galapagos spreading center: Lithospheric	596
	cooling and hydrothermal circulation. <i>Geophysical Journal of</i>	597
	<i>Royal Astronomical Society</i> , <b>38</b> , 587–608.	598
	Wright, J. A., and Loudon, K. E., 1989. <i>Handbook of Seafloor Heat</i>	599
	<i>Flow</i> . Boca Raton: CRC Press. 498 pp.	600
	Yamano, M., Uyeda, S., Aoki, Y., and Shipley, T. H., 1982. Esti-	601
	mates of heat flow derived from gas hydrates. <i>Geology</i> , <b>10</b> ,	602
	339–343.	603
	<b>Cross-references</b>	604
	Heat Flow, Continental	605
	Heat Flow, Continental: Measurement Techniques	606
	Oceanic Lithosphere: Thermal Structure	607

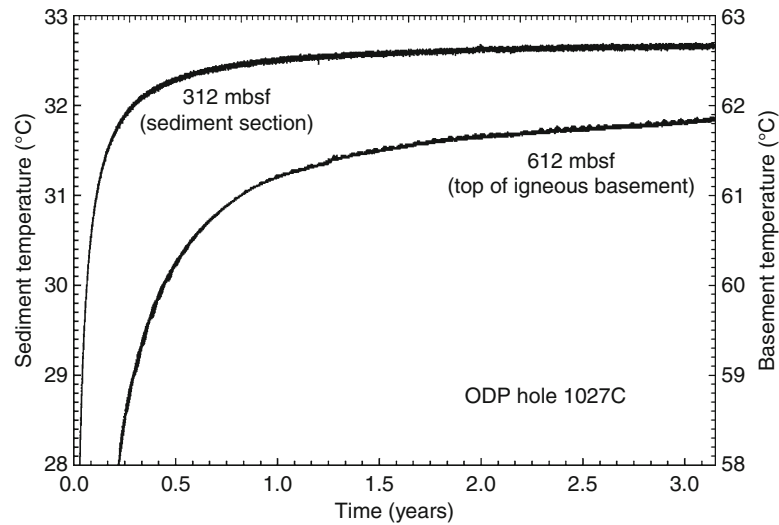


**Seafloor Heat Flow: Methods and Observations, Figure 1** Sensors and probes for measuring temperatures and thermal conductivity in marine sediments, including (a) outrigger temperature sensors mounted to the outside of a sediment corer (core barrel is 12 cm diameter), (b) a devoted heat-flux probe for measuring sediment temperatures and thermal conductivities (total length is 4.5 m), and (c) a high-strength probe that extends below a drill bit for bottom-hole temperature measurements (length is 1.2 m, tip diameter 1 cm).

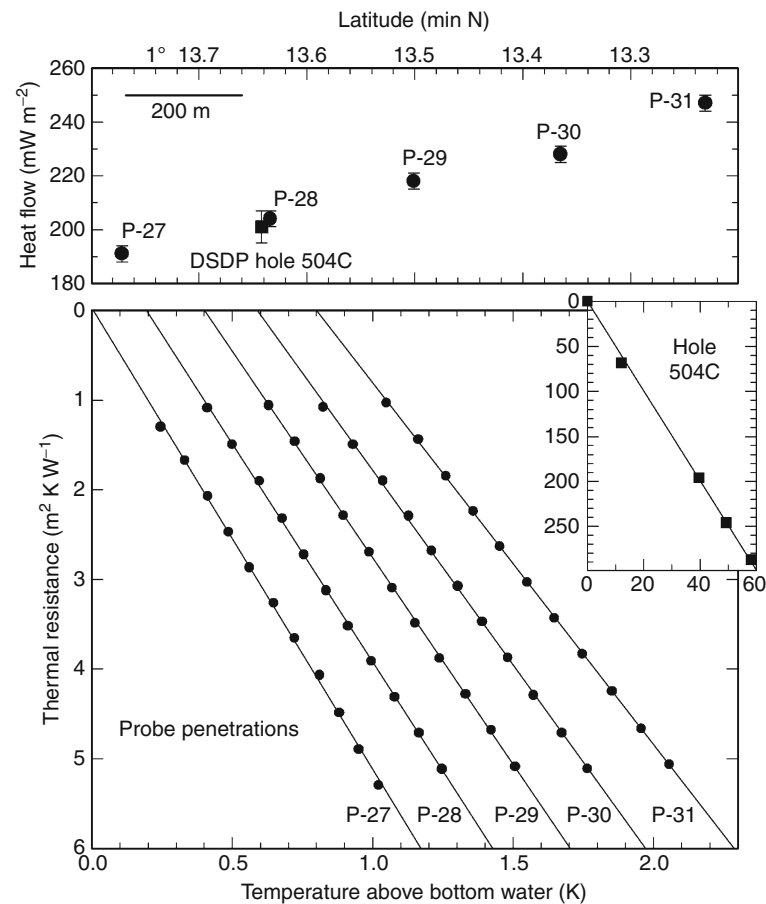


**Seafloor Heat Flow: Methods and Observations,**

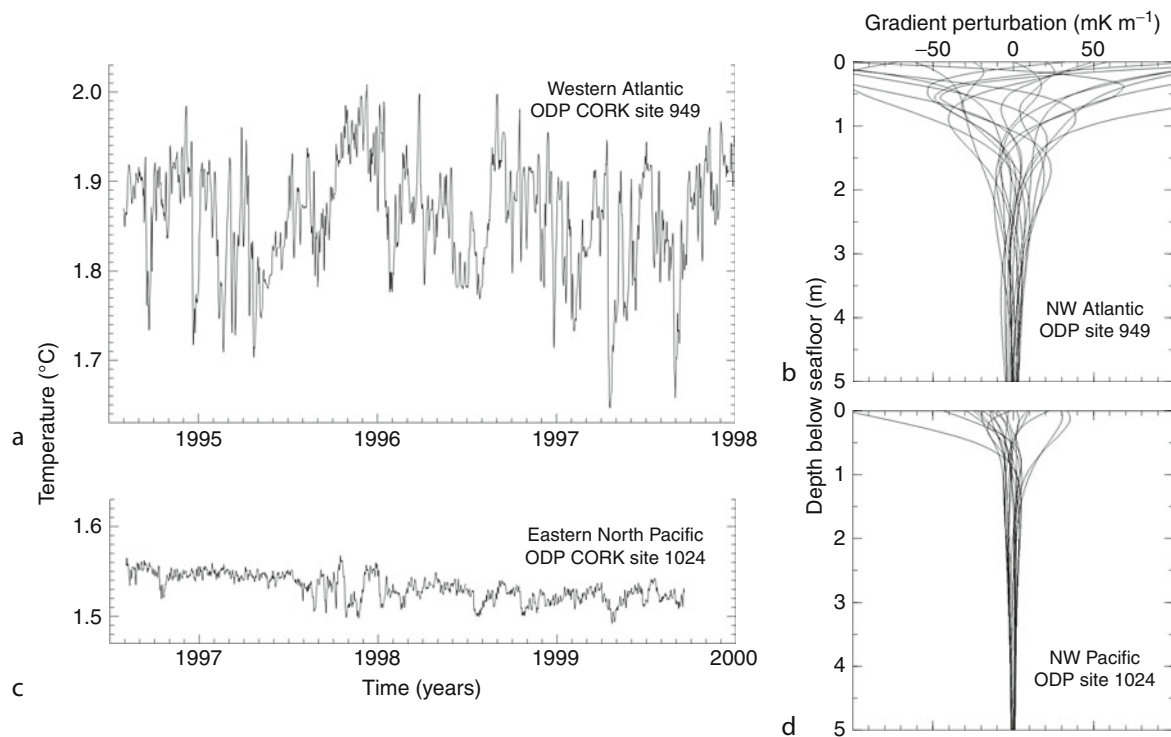
**Figure 2** Typical data (upper panel) collected with a marine heat-flux probe like that shown in Figure 1b. Thermal conductivities are determined from the rates of decay following the metered pulse of heat, and natural sediment temperatures are determined by extrapolating the transients following probe insertion. In this example, high conductivities associated with two turbidic sand layers are present.



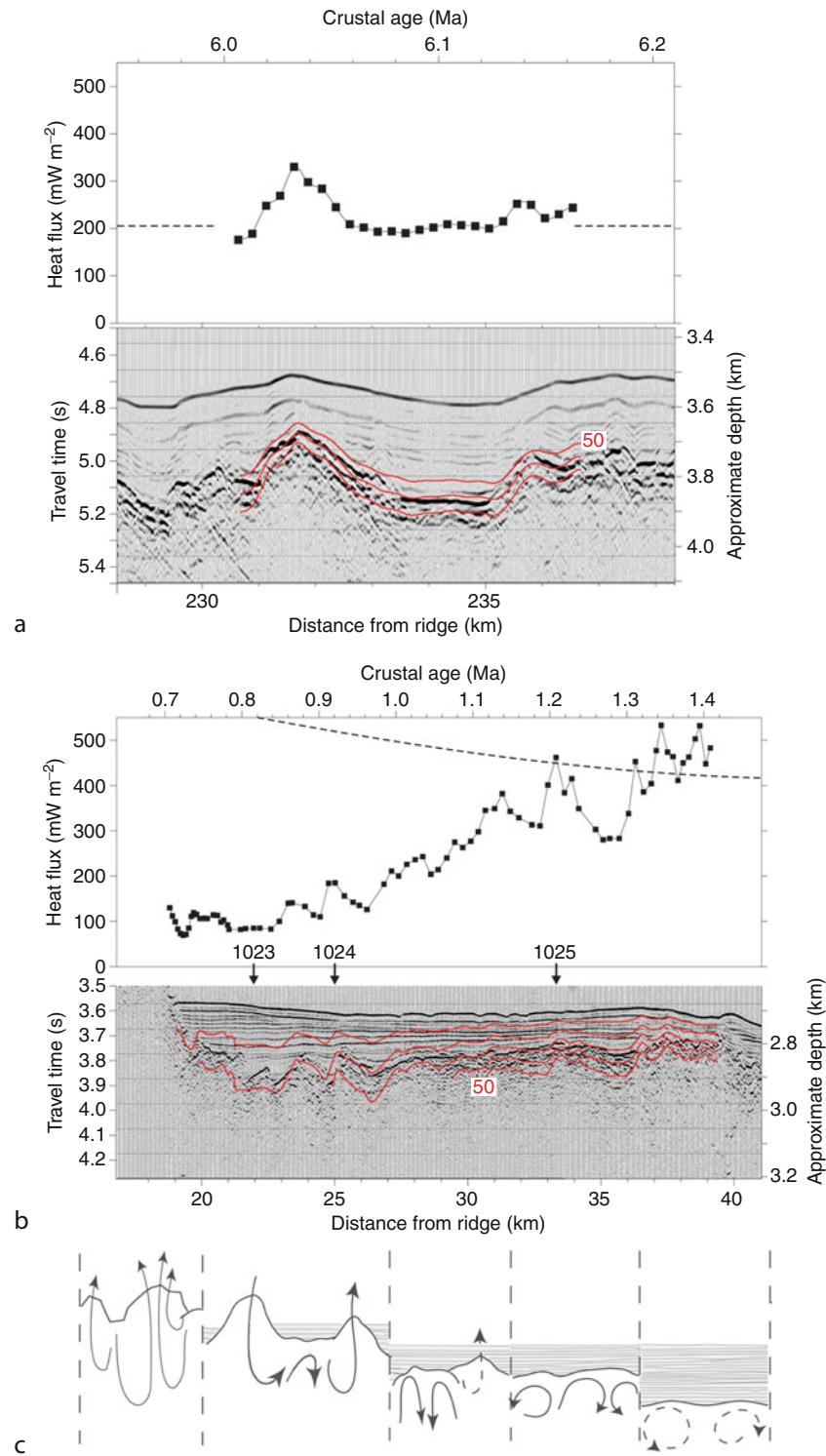
**Seafloor Heat Flow: Methods and Observations, Figure 3** Two records from a 10-thermistor cable suspended in a borehole that penetrates a c. 600-m-thick sediment layer and into the underlying uppermost igneous oceanic crust. The longer recovery time at the deeper level reflects the large volume of water that invaded the uncased and permeable igneous section during the 5 days between the time of drilling and when the hole was sealed and instrumented.



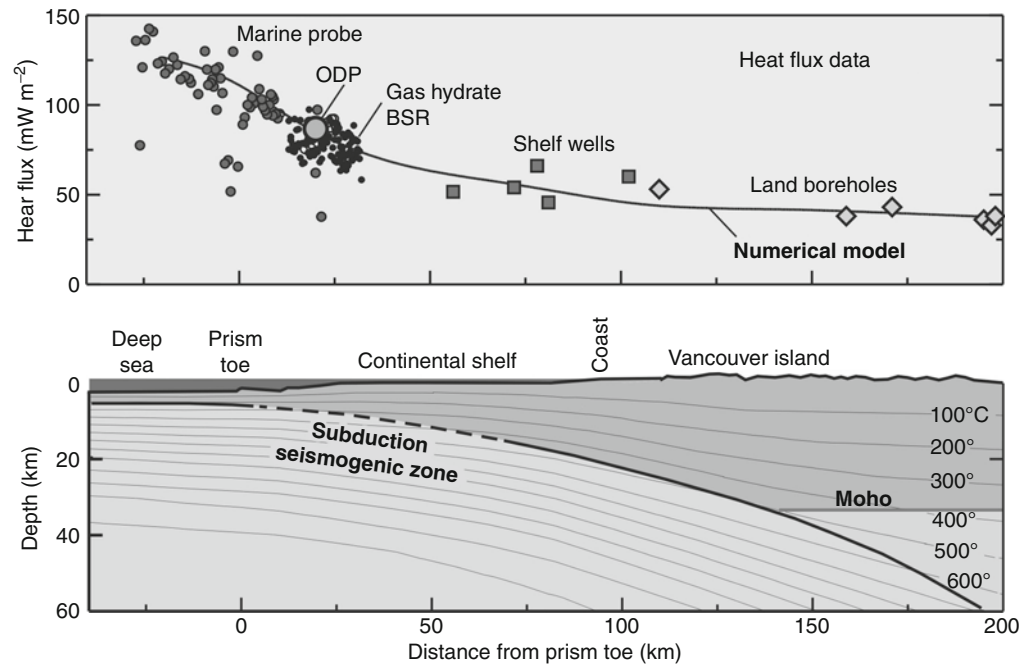
**Seafloor Heat Flow: Methods and Observations, Figure 4** Comparison of collocated seafloor probe and borehole heat-flux observations. Variations in probe measurements along the transect adjacent to the borehole site illustrate how carefully such comparisons must be done.



**Seafloor Heat Flow: Methods and Observations, Figure 5** Bottom-water temperature variations observed in the Atlantic (a) and Pacific Oceans (c), and estimated perturbations of the geothermal gradient as a function of depth (b and d) stemming from the variations, calculated at an evenly distributed suite of times during the temperature time series.



**Seafloor Heat Flow: Methods and Observations, Figure 6** Transects of heat flux on the flanks of the Costa Rica Rift (a) where an extensive sediment cover is present, and Juan de Fuca Ridge (b) striking away from an area of extensive basement at the left end of the figure. Both show the effects of hydrothermal circulation on conductive seafloor heat flux and on the crustal thermal regime. Heat flux estimated on the basis of the local lithosphere age (see text) is shown as the dashed lines. Temperatures estimated below the seafloor are shown at intervals of 10 °C. The cartoons in (c) show the influence of sediment burial on hydrothermal circulation and advective heat loss under a variety of burial states.



**Seafloor Heat Flow: Methods and Observations, Figure 7** Structural and heat-flux transect across the Cascadia subduction forearc, with temperatures estimated from a numerical model for underthrusting and sediment thickening, constrained by the heat-flux data (following compilation of Hyndman and Wang, 1993).